

# Effect of $\text{La}_2\text{O}_3$ Addition on the Thermal, Microstructure and Mechanical Properties of Mullite–Zirconia Composites

H. Aydın

\* hediye.aydin@dpu.edu.tr

Received: December 2018

Revised: March 2019

Accepted: July 2019

Department of Metallurgy and Materials Engineering, Kütahya Dumlupınar University, Kütahya-Turkey.

DOI: 10.22068/ijmse.16.4.10

**Abstract:** Mullite–zirconia composites were prepared using lanthanum oxide ( $\text{La}_2\text{O}_3$ ) additive at three different molar ratios via reaction sintering (RS) of alumina, kaolinite and zircon. Starting materials were planetary milled, shaped into pellets and bars and sintered at a temperature range of 1450–1550 °C with 5 h soaking at peak temperature. Mullite–zirconia composites were characterized in this study by thermal expansion coefficient, physical, microstructural, and mechanical properties. The X-ray diffraction (XRD) method was employed for determining the crystalline phase composition of these composites. Samples with 8 mol%  $\text{La}_2\text{O}_3$  exhibited a flexural strength of ~197 MPa and elastic modulus of 143 GPa. Significant improvements in thermal expansion coefficient were observed in samples with 5 mol%  $\text{La}_2\text{O}_3$ . Composite microstructures were examined via scanning electron microscopy (SEM).  $\text{ZrO}_2$  takes part in both the intergranular as well as intragranular positions. However, intragranular zirconia particles are much smaller compared to intergranular zirconia particles.

**Keywords:** Mullite–zirconia composites, Thermal expansion coefficient, Reaction sintering, Mechanical properties.

## 1. INTRODUCTION

Mullite has excellent characteristics, such as low thermal expansion, high thermal shock resistance and high creep resistance up to 1300 °C. In addition, further improvements in mechanical and thermomechanical properties of mullite can succeed through matrix reinforcement. This is achieved by dispersion of  $\text{ZrO}_2$  particles which results in mullite–zirconia composites [1].

Mullite–zirconia composites have different technically challenging applications due to their superior physicochemical properties such as toughness, chemical stability, and high-creep resistance. They are also employed in the glass industry where a high level of corrosion resistance is required. There are two main solid-state processing routes for manufacturing mullite–zirconia composites: the first is to obtain mullite and then mix it with zirconia powder; while the second is the reaction sintering of a zircon and alumina mixture [2].

The solid-state sintering process requires the transport of atoms from one place to another through diffusion. One of the most important factors that affects the rate and amount of cation dissemination in ionic compounds is the valence/diameter ratio. The field intensities of  $\text{Al}^{+3}$  and  $\text{Si}^{+4}$  ions are high due

to high valence/diameter ratios. This means that these ions pull the anions around them (by polarizing the surrounding oxygen), narrowing the path in the direction of movement thereby making them harder to spread. Due to low and unequal diffusion rates in mullite grains (unit cells) of cations, high temperatures are required to synthesize mullite at high density and to dissolve corundum in mullite grains. In order to synthesize mullite ceramics at or near the theoretical density, sintering is carried out at elevated temperatures (eg. 1650 °C). This difficulty can be overcome by way of various measures and/or controls. Reaction sintering is an easy and inexpensive route to obtain homogeneous mullite–zirconia composites due to the availability of the starting materials and the lower processing temperatures required [3].

Various researchers have studied the effect of different additives on the formation and sintered characteristics of the mullite–zirconia composite. The addition of  $\text{MgO}$  to mullite–zirconia composite is reported to enhance linear shrinkage and falls with the bulk density of sintered samples with increase temperature [4].  $\text{MgO}$  also is reported to improve creep resistance due to the presence of elongated mullite grains [5]. The presence of ulexite and cole-

manite are reported to reduce the decomposition temperature of zircon thereby enabling mullite-zirconia composite synthesis at much lower temperatures [6-7]. SrO additive is reported to have no effect on the phase content of the mullite-zirconia composite [2]. The addition of  $\text{TiO}_2$  to mullite-zirconia composites leads to the change in reaction sintering, densification, and microstructure which can alternately alter the formation temperature and retention of  $t\text{-ZrO}_2$  phase in these composites [8].  $\text{Y}_2\text{O}_3$  is also reported to increase the dissociation of zircon and increase  $t\text{-ZrO}_2$  stabilization through the formation of  $\text{ZrO}_2\text{-Y}_2\text{O}_3$  solid solution [9]. In addition,  $\text{Y}_2\text{O}_3$  improves the thermomechanical properties of the composite [10]. It was found that the addition of lanthanum oxide decreased the densification temperature and significantly improved the thermal shock resistance of the mullite-zirconia composites. Kumar et al. [11] have shown that the addition of  $\text{La}_2\text{O}_3$  to mullite zirconia composites during sintering has significantly improved the thermal shock resistance.

In this study, reaction sintering of mullite-zirconia composite was studied in the presence of lanthanum oxide ( $\text{La}_2\text{O}_3$ ). The novelty of the present work lies in the fact that the starting materials are

usually zircon and alumina in literature. Whereas this study not only dwells in zircon and alumina but also studies the effects of kaolinite as well. The main objective of the present study was to obtain a dense zirconia mullite composite comprised of mullite as the continuous matrix, from inexpensive starting raw materials. For this purpose zircon (as a natural and less-expensive source of  $\text{ZrO}_2$  and  $\text{SiO}_2$ ), commercial-grade calcined  $\text{Al}_2\text{O}_3$  (as a source of  $\text{Al}_2\text{O}_3$ ), and kaolinite ( $\text{Al}_2\text{O}_3\cdot 2\text{SiO}_2\cdot 2\text{H}_2\text{O}$ , as a source of  $\text{Al}_2\text{O}_3$ ) were used to prepare the composite via reaction sintering: 0, 2, 5 and 8 mol % of  $\text{La}_2\text{O}_3$  were used for the synthesis of the product at low temperatures and was considered to be effective on the phase transformation of zirconia in the studies. Finally, sintered composites were characterized in terms of density, thermal expansion hysteresis, phase content, microstructure, and mechanical properties.

## 2. EXPERIMENTAL PROCEDURES

Zircon ( $\text{ZrSiO}_4$ , Johnsen Matthey, Sereltas, Istanbul), kaolinite ( $\text{Al}_2\text{Si}_2\text{O}_5(\text{OH})_4$ , Kütahya-Porselen, Kütahya), alumina ( $\text{Al}_2\text{O}_3$ , Merck, Germany) and lanthanum oxide ( $\text{La}_2\text{O}_3$ , Merck,

**Table. 1.** Chemical and mineral analysis of raw materials

	Zircon	Kaolinite	Alumina
Oxide (wt%)	( $\text{ZrSiO}_4$ )	( $\text{Al}_2\text{Si}_2\text{O}_5(\text{OH})_4$ )	( $\text{Al}_2\text{O}_3$ )
$\text{SiO}_2$	29.96	53.01	0.02
$\text{ZrO}_2$	64.08	-	-
$\text{Al}_2\text{O}_3$	0.02	32.56	95.86
CaO	0.11	0.12	0.49
$\text{B}_2\text{O}_3$	-	-	-
MgO	0.03	0.04	0.02
$\text{Fe}_2\text{O}_3$	0.07	1.16	0.04
$\text{K}_2\text{O}$	0.04	0.13	0.01
$\text{Na}_2\text{O}$	0.11	0.09	0.04
$\text{TiO}_2$	0.22	0.30	0.01
MnO	-	-	-
SrO	0.07	-	-
$\text{HfO}_2$	1.10	-	-
$\text{P}_2\text{O}_5$	1.15	-	-
Major crystalline phases	Zircon	Kaolinite	Corundum

**Table 2.** Batch compositions with codes.

Sample codes	Zircon (wt%)	Kaolinite (wt%)	Alumina (wt %)	Lanthanum oxide with respect to ZrO <sub>2</sub> (mol%)
M0L	30	25	45	-
M2L	32.75	19.98	45.71	1.56
M5L	32	21	44	3
M8L	30	21.09	45.31	3.6

Germany) were used as starting materials. The chemical composition of raw materials used in this study was analyzed via X-ray fluorescence (XRF), the results of which are presented in Table 1. Four batch compositions containing 20 wt.% zirconia and 0, 2, 5 and 8 mol % of lanthanum oxide with respect to zirconia were prepared. The mixtures were marked as M, M2L, M5L, and M8L, respectively (Table 2).

Raw materials were mixed in a pot mill using ZrO<sub>2</sub> grinding media in a methyl alcohol medium for 6 h. Mixed wet mixtures were then dried at 100°C for 24 h. After drying, the mixtures were uniformly mixed with 5 % PVA solution as a binder and shaped into cylindrical pellets (10 mm diameter) for density and microstructure analyses; and rectangular rods with the size of 25 mm × 5 mm × 5 mm and 7.5 mm × 5 mm × 55 mm were pressed at 2 tons for thermal and mechanical characterizations, respectively. The pressed specimens were sintered at 1450, 1500 and 1550 °C for 5 h at a heating rate of 5 °C min.<sup>-1</sup>. Sintered products were characterized for various physical, thermal, mechanical and microstructural properties. Mechanical and thermal properties were measured using all bar samples at 1550 °C. The flexural strengths ( $\sigma$ , MPa) of composites were measured via an Instron 5581 device. In the tests, 2 kN load cell that moved at a rate of 0.5 mm/min. was used. Linear thermal expansion of the samples during

heating-cooling cycles was measured using a dilatometer (model no. NETZSCH DIL 402C). For this purpose, sintered bar samples of the size 25 mm × 5 mm × 5 mm were used.

The bulk density of the samples was measured via the Archimedes' method. Phase analyses were carried out via X-ray diffraction (XRD) technique. The formed crystalline phase was investigated by Panalytical Empyrean X-ray diffractometer using nickel filtered Cu-K $\alpha$  radiation, and diffraction patterns were recorded over a Bragg's angle ( $2\theta$ ) range of 10–60°. Microstructural characterization and energy dispersive X-ray (EDX) analyses were performed via scanning electron microscopy (SEM, FEI Nova NanoSEM, 650) after gold coating.

### 3. RESULTS AND DISCUSSION

#### 3.1. Densification behavior

The variation of density as a function of sintering temperatures and lanthanum oxide content for the different compositions is shown in Table 3. It can be seen that all samples have reached optimum bulk density at a temperature of 1550 °C, but, the effect of lanthanum oxide is prominent at relatively lower temperatures. This is mainly due to the higher affinity of lanthanum oxide to form glassy phases in the presence of Al<sub>2</sub>O<sub>3</sub> and

**Table 3.** Bulk density (g.cm<sup>-3</sup>) of mullite-zirconia composites as a function of lanthanum oxide content and sintering temperature

Sample codes	Temperatures (°C)		
	1450	1500	1550
M0L	2.17	2.26	3.11
M2L	2.67	2.89	3.23
M5L	2.71	3.03	3.35
M8L	3.08	3.25	3.47

SiO<sub>2</sub> [11]. As can be seen from the SEM images, the porosity in the specimens that significantly decreased with controlled amount of La<sub>2</sub>O<sub>3</sub> addition successfully results in the formation of the grains of zirconia at high temperatures while also allowing the formation and considerable growth of mullite. Thus, initially the enhancement of properties takes place. Several researchers [1,2] have reported mullite-zirconia composites with better densification, improved mechanical properties, greater fracture toughness, improved thermal shock resistance, and higher tetragonal zirconia phase content for the La<sub>2</sub>O<sub>3</sub> containing compositions.

### 3.2. Phase analysis

Diffraction patterns of the composites sintered at 1450-1550 °C are shown in Figs. 1-4. Zircon, corundum, m-ZrO<sub>2</sub> and mullite phases observed in XRD patterns belonging to M0L mixture sintered at 1450 °C showed that zircon was partially decomposed and alumina played a significant role in mullite formation. As shown in Fig.1 (1450 °C) M•L mixture is composed of a trace amount of silica and sillimanite. Zircon and corundum phases were found to be present in M0L composition at 1450 °C which indicates that the reaction between these phases has not been completed for the M0L mixture up to a temperature of 1550 °C. The peak intensity of mullite increases from 1450 to 1550 °C, whereas that of corundum, silica, and sillimanite decreases due to mullitization. The corundum phase disappeared at temperatures of 1500 and 1550 °C, while zircon remained partially unreacted [7].

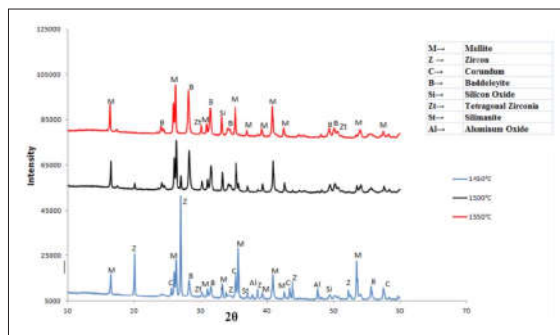


Fig. 1.

XRD patterns for additive-free mixture (M0L) sintered at a temperature of 1450, 1500 and 1550°C.

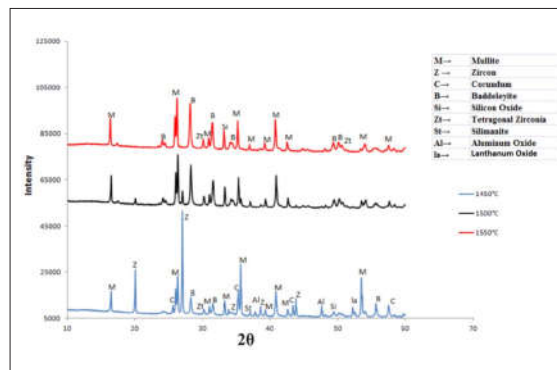


Fig. 2.

XRD patterns for mixture containing lanthanum oxide (M2L) sintered at a temperature of 1450, 1500 and 1550 °C.

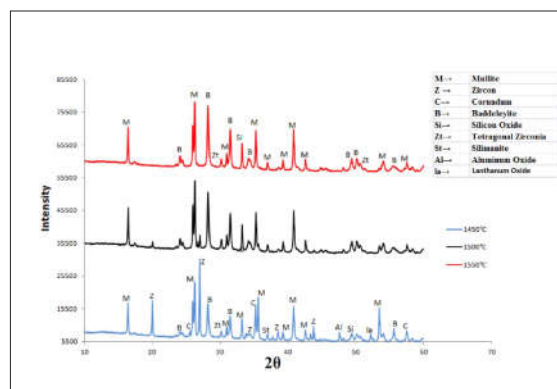


Fig. 3.

XRD patterns for mixture containing lanthanum oxide (M5L) sintered at a temperature of 1450, 1500 and 1550 °C.

Figures 2-4 present the XRD patterns of mullite-zirconia composite sintered at 1500 and 1550 °C for 5 h with different La<sub>2</sub>O<sub>3</sub> concentrations (0, 2, 5 and 8 mol%). For targeted M8L composite, the patterns revealed that addition of La<sub>2</sub>O<sub>3</sub> led to a dramatic drop in the intensity of the unreacted zircon peak in comparison with the La<sub>2</sub>O<sub>3</sub>, M2L, and M5L free sample. On the other hand, there is a remarkable enhancement in the reaction rate especially with the addition 5 mol % La<sub>2</sub>O<sub>3</sub> for samples in addition to a decrease in the alumina content, but alumina still exists as a free phase at 1450 °C. Increasing La<sub>2</sub>O<sub>3</sub> content to 8 mol % led to a complete vanishing of the zircon peak.



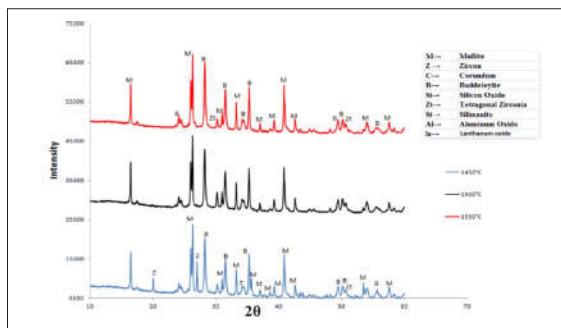


Fig. 4.

XRD patterns for mixture containing lanthanum oxide (M8L) sintered at a temperature of 1450, 1500 and 1550 °C.

However, the disappearance of zircon in the presence of lanthanum oxide can be attributed to two reasons. The first possible reason is the sintering time, while the second is the sintering temperature. Zircon is decomposed into crystalline zirconia and unreacted free amorphous silica. This implies that either sintering temperature (1550 °C) and/or sintering time (5 h) is not sufficient. Diffractograms of the sintered specimens are given in in Fig. 1-4 for 1550 °C, where the highest peaks of tetragonal (t-ZrO<sub>2</sub>) and monoclinic (m-ZrO<sub>2</sub>) phase are located. The t-ZrO<sub>2</sub> and m-ZrO<sub>2</sub> phases are observed for each mixture. The dominance of monoclinic zirconia phase in XRD analysis can be attributed to two reasons. The first possible reason is the large size of the tetragonal zirconia particles and the second is the dissolving of La<sub>2</sub>O<sub>3</sub> in mullite structure rather than the zirconia structure. It is related to the particle size of zirconia whether the high temperature tetragonal (and cubic) zirconia phase is reconverted into the monoclinic phase at room temperature or not. It is indicated in many sources that tetragonal zirconia is converted to its monoclinic phase at room temperature if it is pure and above a certain (critical) dimension. [12-14].

### 3.3. Microstructures

SEM photomicrographs of all samples sintered at 1450-1550 °C are shown in Figs. 5-8. M0L, M2L, and M5L samples present high porosity at lower sintering temperatures and appear to be dense microstructure with increasing sintering temperatures. It has been determined based on SEM photomicrographs of mullite-zirconia compacts that Mullite exhibits equiaxed grains in all samples sintered at

1550 °C. Mullite grains are equiaxed in nature, but they are observed as elongated grains in microstructure photographs due to the impact of La<sub>2</sub>O<sub>3</sub> development. The zirconia grains were distributed throughout the mullite matrix. Two types of zirconia grains were observed to be available; one is the inter-granular t-ZrO<sub>2</sub> located between the mullite grains and the other is the intra-granular t-ZrO<sub>2</sub> located inside the mullite grains. Intra-granular ones are much smaller than the inter-granular zirconia grains. The presence of a liquid phase extremely expedites the growth of inter-granular ZrO<sub>2</sub> grains. The increase in La<sub>2</sub>O<sub>3</sub> content and sintering temperature assisting the increase in zirconia grain size can be attributed to the generation of the transitory liquid phase that promotes grain growth in the liquid state at high temperature [15-16] which made the comparison between M0L and M8L sintered at 1550 °C (Fig. 5c and Fig. 8c) for the effect of La<sub>2</sub>O<sub>3</sub> content.

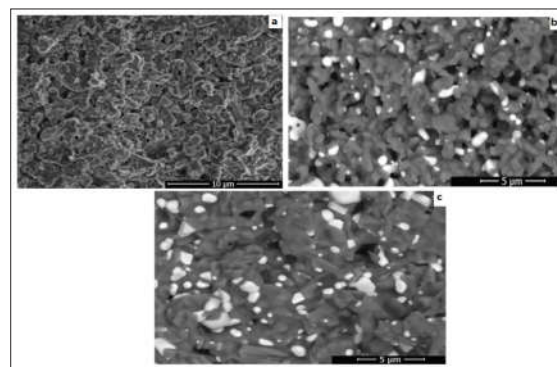


Fig. 5.

Microstructure of M0L mixture sintered at a temperature of 1450°C (a), 1500°C (b) and 1550°C (c).

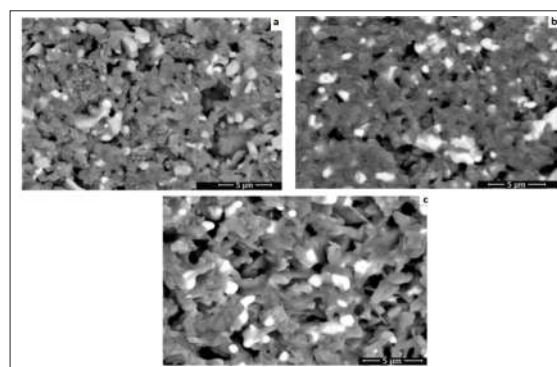


Fig. 6.

Microstructure of M2L mixture sintered at a temperature of 1450°C (a), 1500°C (b) and 1550°C (c).

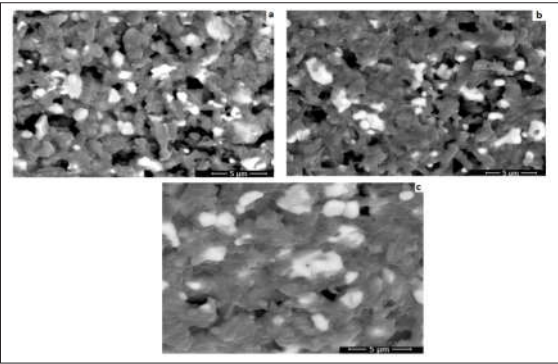


Fig. 7.

Microstructure of M5L mixture sintered at a temperature of 1450°C (a), 1500°C (b) and 1550°C (c).

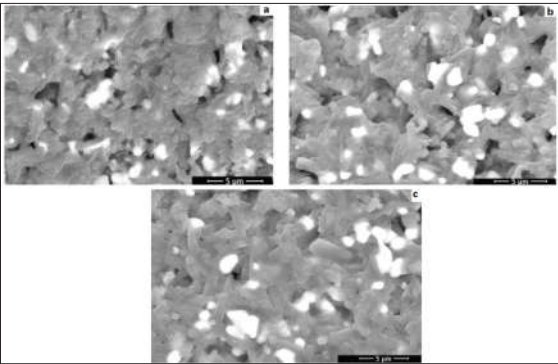


Fig. 8.

Microstructure of M8L mixture sintered at a temperature of 1450°C (a), 1500°C (b) and 1550°C (c).

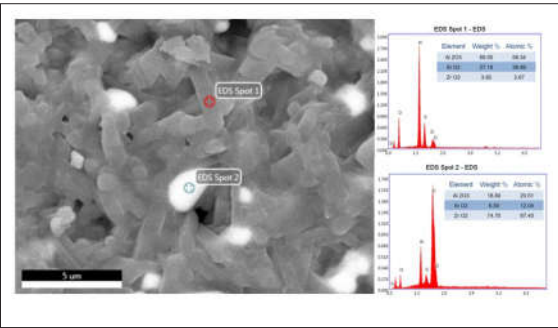


Fig. 9.

SEM photomicrograph and corresponding EDX spectra of the sample M8L sintered at 1500°C: (EDS Spot 1) Mullite grain and (EDS Spot 2) zirconia grain

Figure 9 shows the SEM photomicrograph and the corresponding EDX spectra for the M8L sample sintered at 1550 °C. Accordingly, EDS Spot 1 specifies mullite grain (dark grain) and EDS Spot 2 specifies zirconia grain (bright grain). These mi-

crostructure images reveal that the almost-dense mullite–zirconia composites are formed in the M8L sample sintered at 1550 °C.

3.4. Mechanical properties (E and  $\sigma$ )

Elastic modulus (E, GPa) and flexural strength ( $\sigma$ , MPa) values of composites sintered at 1450, 1500 and 1550 °C are given in Tables 4 and 5, respectively. As was the case in our previous studies [7], the average and standard errors of RT flexural strength correspond to at least five tests for each growth rate. Table 4 shows the variation of high-temperature flexural strength of samples with different  $\text{La}_2\text{O}_3$  content as a function of temperature. All samples displayed almost similar variations in flexural strength with temperature. Afterward, the flexural strength increases with the increasing lanthanum oxide additive and the temperature (from 1450 °C to 1550 °C) due to highly viscous glassy phases [11]. The influence of lanthanum oxide addition of mullite-zirconia composites can be described as follows: when it acts as an additive (very low concentrations) the values of the elastic modulus and flexural strength are slightly increased. These values are slightly lower than those provided in literature for pure mullite (254 MPa), mullite–zirconia (about 215 MPa), and pure zircon (150–320 MPa) for several products sintered at 1600 °C. The differences in the flexural strengths of these composites correspond with the density, porosity and phase compositions [8, 17-19].

Table 4. Flexural strength ( $\sigma$ , MPa) of compositions sintered at 1450, 1500 and 1550 °C

Temperature (°C)	M0L	M2L	M5L	M8L
1450	63	100	116	129
1500	108	117	123	142
1550	166	179	190	197

Table 5. Elastic modulus (E, GPa) of compositions sintered at 1450, 1500 and 1550 °C

Temperature (°C)	M0L	M2L	M5L	M8L
1450	34	83	85	105
1500	72	85	92	113
1550	92	119	131	143

The elastic modulus values obtained are almost close to those of pure zirconia and pure mullite ceramics (200 GPa and 204 GPa respectively) [11]. Indestructible porosity of the composites is probably the main cause of the low measured modulus as mentioned in literature [12]. Flexural strength and elastic modulus values increased almost linearly with increasing lanthanum oxide content and sintering temperature. This might be related to the formation of more elongated and inter-locked mullite and homogeneously distributed intergranular (between mullite grains) and intra-granular (within mullite grains) zirconia particles in the microstructure.

### 3.5. Linear thermal expansion behavior of composites

Linear thermal expansion analysis was used to arrange the correlation between the formed phases and their contents on the expansion behavior of the mullite-zirconia composites. This test was performed using dilatometry (Netzsch Dil. 402 PC, Germany). Linear thermal expansion of the fired compacted mullite-zirconia composites with and without lanthanum oxide additive sintered at 1550 °C, during heating-cooling cycle has been illustrated in Fig. 10. It was also observed in our study at a temperature of around 1100 °C in accordance with the studies by Sarkar et al. (2006), Kumar et al. (2015) and Hemraet et al. (2014), that a sudden narrowing during heat-

ing and sharp expansion during cooling mark the  $Z_m \rightarrow Z_t$  and  $Z_t \rightarrow Z_m$  phase transformations of  $ZrO_2$ , respectively [1, 19, 20]. The hysteresis loop at that region is related to the stabilization of zirconia. Hysteresis area of the curve is higher for M5L and decreased for the samples containing 2 mol% lanthanum oxide (M2L), after which the hysteresis area is almost the same for the sample M8L indicating that stabilization of tetragonal zirconia content is optimum for the samples containing 5 mol% lanthanum oxide.

Partially stabilized zirconia has a lower coefficient of thermal expansion than the fully stabilized zirconia [19]. The presence of  $La_2O_3$  stabilizes t- $ZrO_2$  at room temperature and reduces the sudden volume change of the samples at around 1100 °C, which is confirmed by the reduced hysteresis area of the samples containing  $La_2O_3$  during heating-cooling cycle as shown in Fig. 10. Also, the coefficient of thermal expansion (CTE) has been decreased from  $5.4766 \times 10^{-6} K^{-1}$  (for sample M0L) to  $5.0258 \times 10^{-6} K^{-1}$  (for sample M5L) with addition of  $La_2O_3$ . Dilatation of M0L presented a linear change with temperature; the thermal expansion coefficient up to 1450 °C was  $\approx 5.4766 \times 10^{-6} K^{-1}$  for the sample sintered at 1550 °C. M2L, M5L, and M8L also displayed a linear curve, and thermal expansion coefficients of up to 1450 °C were  $\approx 5.2780 \times 10^{-6} K^{-1}$ ,  $\approx 5.0258 \times 10^{-6} K^{-1}$ , and  $\approx 5.2598 \times 10^{-6} K^{-1}$  for the samples sintered at 1550 °C, respectively.

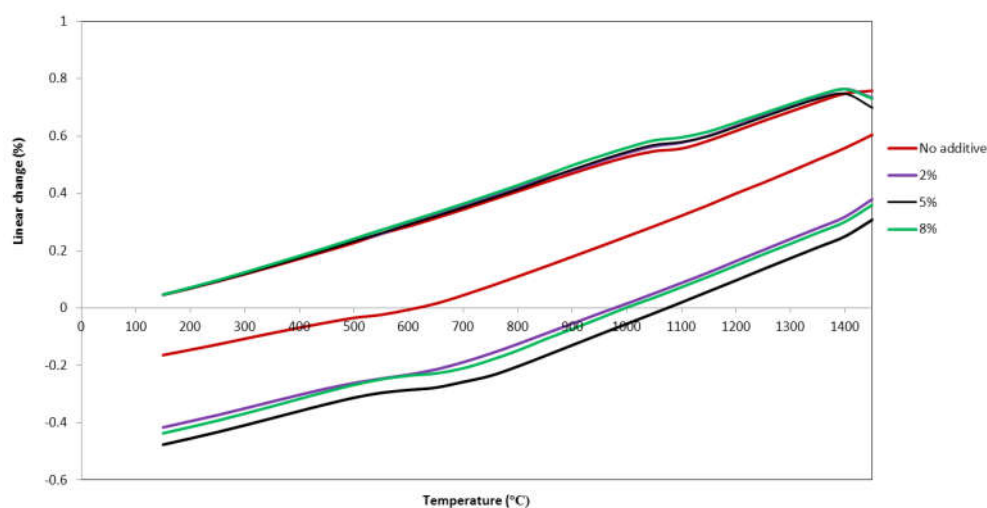


**Fig. 10.** Linear thermal expansion of the mullite-zirconia composites with and without lanthanum oxide additive sintered at 1550 °C during heating-cooling cycle.

#### 4. CONCLUSIONS

The present study reports the production and characterization of mullite-zirconia composites synthesized by reaction sintering of zircon, alumina, and kaolinite in the presence of lanthanum oxide ( $\text{La}_2\text{O}_3$ ) at a temperature range of 1450-1550 °C. The effects of various amounts of  $\text{La}_2\text{O}_3$  additive on the properties of the composites were studied in this study. Density, as well as flexural strength and elastic modulus of composites, increased linearly with lanthanum oxide content in the mixture. These composites had bulk densities of 2.17-3.47 g cm<sup>-3</sup>. It has been shown that addition of  $\text{La}_2\text{O}_3$  increases the reaction sintering process and decreases the final sintering temperature with the appearance of a transitory liquid phase. Several researchers studied the effects of  $\text{Fe}^{3+}$  and  $\text{Ta}^{5+}$  ions on the sintering characteristics of yttria-stabilized zirconia (YSZ) [21]. They reported that  $\text{Fe}^{3+}$  and  $\text{Ta}^{5+}$  ions increase the jump frequency of  $\text{Zr}^{4+}$  ions by decreasing the activation energy, thus increasing the densification rate of YSZ bodies. Since  $\text{Zr}^{4+}$  (~ 0.72 Å) and  $\text{O}^{2-}$  (~ 1.4 Å) ions are smaller than  $\text{La}^{3+}$  (~ 1.05 Å) ions, the addition of  $\text{La}^{3+}$  ions into mullite- $\text{ZrO}_2$  composites in this study, distorted the crystallite structure, resulting in the formation of defects. Similar to the  $\text{Fe}^{3+}$  and  $\text{Ta}^{5+}$  induced defects of YSZ, the defects caused by  $\text{La}^{3+}$  enhance the diffusion rate of ions [21, 22]. It is thought that the anion vacancies diffused because of  $\text{La}^{3+}$  ions can partially substitute  $\text{Zr}^{4+}$  ions [23].  $\text{La}_2\text{O}_3$  doping weakens the Zr-O bond because  $\text{Zr}^{4+}$  (~ 0.72 Å) and  $\text{Si}^{4+}$  (~ 0.9 Å) are smaller than  $\text{La}^{3+}$ . The weak Zr-O bond decreases the activation energy and accelerates the densification rate of mullite- $\text{ZrO}_2$  composites [22].

XRD analysis indicated similar phases for all the compositions sintered at different temperatures; with only a marginal increase in the peak intensity of the samples sintered at higher temperatures. The qualitative phase analysis study of these composites showed similar phases for all the composites sintered at 1450-1550 °C; no difference in phase content was observed, except for a prominent increase in the peak intensity for the samples sintered at

higher temperatures. It is highly possible that impurities sourced from the use of natural raw materials will dissolve in the first formed mullite phase. Since impurities are dissolved in the first formed mullite and glassy/liquid silica phase, the amount of dissolution of the impurities in the zirconia phase is very low. Therefore, the amount of stable or semi-stable zirconia phases in sintered products is very low.

It can be said that the flexural strength of mullite-zirconia composites was improved when more lanthanum oxide content was added and the sintering temperature was between 1450 and 1550 °C. Lanthanum oxide was reported to form a silica-rich glassy phase that ejected out from the bulk of the ceramic during sintering, thereby minimizing the retention of the glassy phase at the grain boundaries and improving the mechanical properties [11, 24]. The maximum flexural strength of the samples containing 2, 5 and 8 % lanthanum oxide were 179, 190, and 197 MPa, respectively. It can be seen that samples with and without  $\text{La}_2\text{O}_3$  additive have displayed nearly equal flexural strength values at room temperature.

As a parallel to similar work in literature [2,11,25] M0L-M8L composites put forth a linear expansion curve with similar linear expansion coefficients, ( $\approx 5.2 \times 10^{-6} \text{ K}^{-1}$ ) excluding the M0L composition which presented a hysteresis loop area, due to the volume change associated to the  $m \leftrightarrow t$  transformation. The  $m \leftrightarrow t$  transformation began at 1100 °C on heating and indicated that an important content of  $m\text{-ZrO}_2$  was present. There is little difference in transformation temperatures among the mixtures without  $\text{La}_2\text{O}_3$ , with 5 mol%  $\text{La}_2\text{O}_3$  and with 8 mol%  $\text{La}_2\text{O}_3$  (Fig. 10). However, the area under the hysteresis loop decreases with an increasing amount of  $\text{La}_2\text{O}_3$  content. This might be due to the presence of a lesser amount of monoclinic zirconia ( $m\text{-ZrO}_2$ ) phase in the  $\text{La}_2\text{O}_3$  containing sintered products. In this way, increasing the amount of  $\text{La}_2\text{O}_3$  results in better retention of the tetragonal phase. This may be due to the solid solution of  $\text{La}^{3+}$  in  $\text{Zr}^{4+}$ , as has been observed for  $\text{Y}^{3+}$  in  $\text{Zr}^{4+}$  by Das et al [1,10].

Mullite and  $\text{ZrO}_2$  showed grains with inhomogeneous size and morphology. These microstructures two main phases have appeared,



mullite (dark grains) and zirconia (bright grains). Zirconia grains have occupied the intergranular as well as intragranular positions in the mullite matrix. It can be observed that the addition of increasing amounts of  $\text{La}_2\text{O}_3$  into the mullite-zirconia composites slightly altered their microstructure. The growth of elongated mullite became more pronounced with the use of  $\text{La}_2\text{O}_3$ , and increased with increasing liquid phase formed [25]. Especially, the addition of 8 mol%  $\text{La}_2\text{O}_3$  significantly enhances the microstructure of different composites through reduction of porosity than in case of composites without  $\text{La}_2\text{O}_3$ . The liquid phase formed supports the reduction of porosity and enhances densification level of composites while it was also determined that the incorporation of zirconia in the mullite matrix enhances its mechanical properties, especially its flexural strength and elastic modulus.

It can be said that mullite zirconia composites with  $\text{La}_2\text{O}_3$  additive displayed the best linear expansion coefficient which may be related to the microstructural characteristics achieved via reaction sintering process. The resulting microstructure possessed optimal features such as a uniform distribution of the fine intragranular zirconia ( $\text{t-ZrO}_2$ ). Crack propagation was prevented possibly as a result of matrix compression due to the amount of transformable tetragonal phase. Moreover, the presence of anisotropic (elongated) mullite crystals can also deflect crack propagation [25].

#### Compliance with ethical standards

**Conflict of interest** The author declared that they have no conflict of interest in this work.

#### REFERENCES

1. Sarkar, R. Ghosh, Halder, A. M. K. Mukherjee, B. and Das, S. K. "Effect of Lanthanum oxide on reaction sintering of zirconia-mullite composites", *American Ceramic Society Bulletin*, 2006, 85 (1), 9201-9205.
2. Sarkar, Bishoyi, R. K. "Reaction sintering of zirconia-mullite composites in presence of  $\text{SrO}$ ", *Interceram Refractories Manual*, 2014, 63 (6) 304-306.
3. Aydın, H., "Synthesis of Mullite/Zirconia Composite Materials Doped with Boron Minerals", Ph.D. Thesis, Dumlupınar University, Turkey, 2003.
4. Halder, M. K., "Effect of magnesia additions on the properties of zirconia-mullite composites derived from sillimanite beach sand", 2003, 29, 573-581.
5. Pena, Moya, P. J. S. Aza, S. Cardinal, E. Cambier, Leblud, Anseau, F. C. M. R. "Effect of magnesia additions on the reaction sintering of zircon/alumina mixtures to produce zirconia toughened mullite", *Journal of Materials Science Letters*, 1983, 2, 772-774.
6. Aydın, H. Gören, R. "Effect of ulexite on thermal and mineralogical properties of Mullite-zirconia composite", *Journal of Australian Ceramic Society*, 2017, 53, 2, 283-286.
7. Aydın, H. Gören, R., "Effect of colemanite on properties of traditional mullite zirconia composite Cogent Engineering", *Cogent Engineering*, 2016, 3: 1209809, 1-10.
8. Ebadzadeh, T., Ghasemi, E., "Ceramics International, 'Effect of  $\text{TiO}_2$  addition on the stability of  $\text{t-ZrO}_2$  in mullite- $\text{ZrO}_2$  composites prepared from various starting materials", 2002, 22, 447-450.
9. Halder, M. K., Pal, T. K., Banerjee, G., "Preparation and properties of  $\text{Y}_2\text{O}_3$  containing zirconia-mullite composites derived from sillimanite beach sand", *Ceramics International*, 2002, 28, 311-318.
10. Das, K., Banerjee Mukherjee, G. B., "Effect of Yttria on Mechanical and Microstructural Properties of Reaction Sintered Mullite-Zirconia Composites", *Journal of the European Ceramic Society*, 1998, 18, 1771-1777.
11. Kumar, P., Nath, M. A., Ghosh, H. S., Tripathi, "Thermo- mechanical properties of mullite-zirconia composites derived from reaction sintering of zircon and sillimanite beach sand: Effect of  $\text{CaO}$ ", *Materials Characterization*, 2016, 26, 2397-2403.
12. Rendtorff, N. M., Garrido, L. B., Aglietti, E. F., "Zirconia toughening of mullite-zirconia-zircon

- composites: properties and thermal shock resistance", *Ceram. Int.*, 2009, 33, 7, 311-318.
13. Garrido, L. B., "Hardness and fracture toughness of mullite-zirconia composites obtained by slip casting", *Material Science and Engineering*, 2006, A 419, 290-296.
  14. Zhao, S., Huang, Y. and Wang, C., "Mullite formation from reaction sintering of  $ZrSiO_4/\alpha-Al_2O_3$  mixtures", 2003, *Materials Letters*, 57, 1716-1722.
  15. Haldar, M. K. and Banerjee, G., "Effect of magnesia additions on the properties of zirconia-mullite composites derived from sillimanite beach sand", *Mater. Lett.*, 2003, 57, 3513-3520.
  16. Wei, W. C. J., Kao, H. C. and Lo, M. H., "Phase transformation and grain coarsening of zirconia/mullite composites", *Eur. Ceram. Soc.*, 1996, 16, 239-247.
  17. Rendtorff, N. M., Garrido, L. B. and Aglietti, E. F., "Thermal shock behavior of dense mullite-zirconia composites obtained by two processing routes", *Materials Science and Engineering A*, 2008, 498, 208-215.
  18. Hamidouche, M., Bouaouadja, N., Olagnon, C. and Fantozzi, G., "Thermal shock behavior of Mullite ceramic", *Ceram. Int.*, 2003, 29, 599-609.
  19. Kumar, P., Nath, M., Ghosh, A. and Tripathi, H. S. "Synthesis and characterization of mullite-zirconia composites by reaction sintering of zircon flour and sillimanite beach sand", *Bull. Mater. Sci.*, 2015, 38, 6, 1539-1544.
  20. Hemra, K. and Aungkavattana, P., *Advances in Applied Ceramics*, 2014, 113, 6, 323-329.
  21. Guo, F. and Xiao, P., "Effect of  $Fe_2O_3$  doping on sintering of yttria-stabilized zirconia", *J. Eur. Ceram. Soc.* 2012, 32, 4157-4164.
  22. Sui, Y., Han, L. and Jiang, Y., "Effect of  $Ta_2O_5$  addition on the microstructure and mechanical properties of  $TiO_2$ -added yttria-stabilized zirconia-toughened alumina (ZTA) composites", *Ceramics Int.*, 2018.05, 112.
  23. Skinner, Stephen J., Kilner, John, A., "Oxygen ion conductors", *Materials Today*, 2003, 6, 30-37.
  24. Rendtorff, N. M., Liliana, B. and Aglietti, E. F., "Thermal shock behavior of dense mullite-zirconia composites obtained by two processing routes", *Ceramics International*, 2008, 34, 2017-2024.
  25. Ji, H., Fang, M., Huang, Z., Chen, K., Xu, Y., Liu, Y. and Huang, J., "Effect of  $La_2O_3$  additives on the strength and microstructure of mullite ceramics obtained from coal gangue and  $\gamma-Al_2O_3$ ", *Ceram. Int.* 2013, 39, 6841-6846, 239-247.